

## Aerodynamics of Sport Balls, Badminton Shuttlecock and Javelin

Rakhab C. Mehta<sup>1\*</sup>

<sup>1</sup>Noorul Islam Centre for Higher Education, Kumarcoil, Tamilnadu, India

DOI: 10.36347/sjet.2023.v11i02.001

| Received: 04.01.2022 | Accepted: 08.02.2023 | Published: 12.02.2023

\*Corresponding author: Rakhab C. Mehta

Noorul Islam Centre for Higher Education, Kumarcoil, Tamilnadu, India

### Abstract

### Original Research Article

The focus of the present chapter is to analysis aerodynamic forces and moment on sport balls, badminton shuttlecock and javelin. Lift force is analytically obtained employing Kutta-Joukowski theorem over a spinning sphere in an inviscid and incompressible flow. The inviscid flow analysis reveals that lift force is directly proportional to spinning which coincides with the experimental data of Bearman and Harvey. The lift force over the spinning sphere is less as compared to a rotating cylinder. The tangential velocity component on the surface of the spinning sphere is a cubic algebraic equation which has one real and two conjugate imaginary roots. Aerodynamic performance of feather and synthetic badminton shuttlecock is discussed in conjunction with experimental data. Available video images of a javelin trajectory are used to reconstruct its aerodynamic performance.

**Keywords:** Aerodynamic, CFD, drag, javelin, lift, inviscid flow, mathematical modelling, shuttlecock, sport ball, trajectory, wind tunnel, spin, Magnus effect, pitching moment.

Copyright © 2023 The Author(s): This is an open-access article distributed under the terms of the Creative Commons Attribution 4.0 International License (CC BY-NC 4.0) which permits unrestricted use, distribution, and reproduction in any medium for non-commercial use provided the original author and source are credited.

## 1. INTRODUCTION

Aeronautical, mechanical, biomedical and computer science and engineering are playing a vital role for better understanding of sports science. Books on baseball [1], sports ball [2], football [3], soccer [4], projectiles in sport [5, 6], biomechanics [7] and biological data [8] are published to study sport science and engineering. Many review articles have appeared describing the aerodynamics characteristic sport projectiles [9-12] and neural network model [13] of athletes. Recently published paper [14] presents an interesting 2-Dimensional analysis of a badminton shuttlecock for re-entry vehicle application.

Fluid mechanics [15] in conjunction with flight dynamics [16] are employed to determine the aerodynamic forces, moment and trajectory of soccer, badminton shuttlecock and javelin. Inviscid flow analysis predicts the lift force over a spinning cylinder and sphere. However, a viscous flow forms a boundary layer [17, 18] over the sport balls that significantly affect aerodynamic forces such as lift [19] and drag [20].

The sport aerodynamics mainly deals with the aerodynamic analysis and performance assessment of different sports ball shuttlecock and javelin using wind tunnel testing and CFD methods. Wind tunnel testing [21, 22] is required to understand flow field over a

sports ball at different Reynolds number and spinning rate. The wind tunnel balance was originally built to measure the drag, lift and pitching moment. The smoke flow visualization experiments and PIV analysis were performed to make the flow pattern visible around the cricket ball [23], tennis ball [12], golf ball [24], ping pong [25], badminton shuttlecock [26]. Wind tunnel measurements of aerodynamic forces on a football is conducted by Rae *et al.*, [27].

Aerodynamic forces are measured by Daish [2] from a deviating golf ball at a normal velocity of 32 m/s and spinning speed less than 5000 rpm. A Magnus force on a smooth spinning ball of 15.2 cm (6") diameter in a wind tunnel was instinctively measured by Maccoll [28]. Briggs [29] has measured pressure distribution over a smooth ball of 7.62 cm (3") diameter at spin rates up to 1800 rpm at freestream velocity of 38 m/s (125 ft/s) at Reynolds number of  $2.4 \times 10^5$  based on ball diameter. Briggs [29] has measured the lateral deflection and was proportional to  $\omega V_\infty^2$ . Pressure at the equatorial surface over the spinning sphere was measured by Briggs [28] and found that the resultant pressures are consistently in accord with the Magnus effect [30].

The application of the commercial CFD, FLUENT, to sports ball aerodynamics was assessed and validated using 3D analysis technique for sports balls in

conjunction with a 3D laser scanner or drawn in CAD. Powerful software packages like, for example, Mathematica and Maple. A comprehensive survey of computational fluid dynamics (CFD) approach is presented by Hanna [31].

A numerical study of the erratic motion of soccer balls is carried out by Barber *et al.*, [32]. Numerical flow simulations over baseball, soccer ball and volleyball are performed to find out aerodynamic characteristics [33]. Large eddy simulation of the flow over a soccer ball is done by Iftikhar *et al.*, [34]. Numerical simulation of flow over a stationary and rotating sphere is carried out by Poon *et al.*, [35]. CFD

approach is applied to study aerodynamics of a Ping Pong in free flight by Ou *et al.*, [25]. Verma *et al.*, [36] carried out CFD simulations of badminton shuttlecocks.

## 2. FLUID MECHANIC AND FLIGHT DYNAMIC IN SPORTS

Basic Aerodynamic principles initially assume the flight of a smooth sphere through an inviscid flow. D'Alembert's Paradox [15] is the inference that the drag on a body moving steadily through an inviscid fluid must vanish. The sensitivity of the aerodynamic force to the drag crisis plays a critical-role in a number of ball sports.

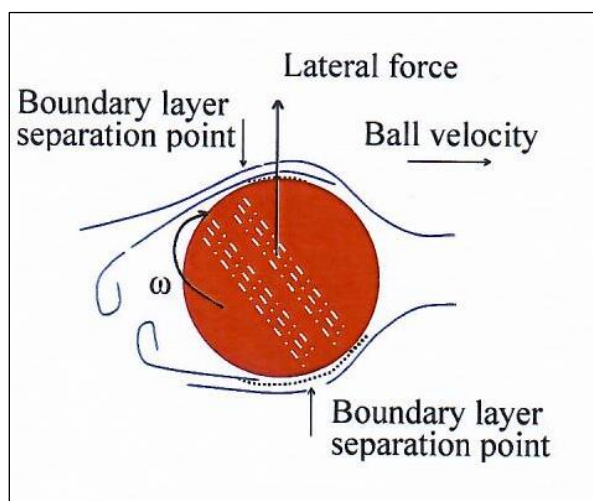


**Fig 1: Reverse swing on a high velocity cricket ball**

But in a viscous fluid such as air, a thin boundary layer [18] is formed around the sphere and its nature depends on pressure gradient, spin parameter,  $S = \Omega d/V$  and Reynolds number,  $Re = \rho V d/\mu$ , ( $4.0 \times 10^4 - 4.0 \times 10^5$ ) based on diameter of the sphere, where  $\Omega$ ,  $V$ ,  $d$ ,  $\rho$ , and  $\mu$  are angular velocity, fluid velocity, diameter, density of fluid and molecular viscosity, respectively. The boundary layer separating from the ball is a mixing of the shed layer and the inviscid free-flow region. Figure 1 illustrates the flow field over a cricket ball. Using Newton's second law of motion to describe the fluid element and considering the

fluid element's volume to make-up part of a fluid continuum, one arrives at the Navier–Stokes equations [18]. CFD simulation to these equations yields a velocity field around balls as a function of  $Re$  and  $S$  for most sport balls or projectiles. Note that the boundary layer separates farther back on the ball from turbulent flow compared to laminar flow. Recent research [37–39] has been done to understand how spinning, surface geometry and roughness changes aerodynamic coefficients. Figure 2 shows flow features over a spinning ball.

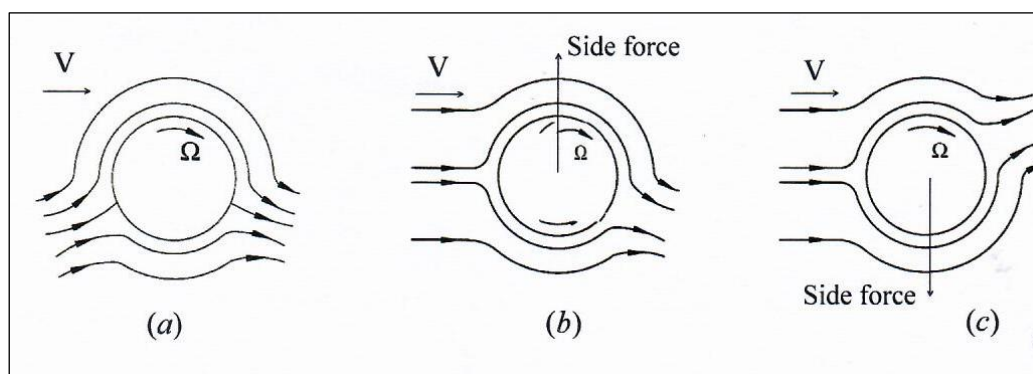


**Fig 2: Flow pattern for a ball combined with viscous and circulating flow**

Figure 3 illustrates the asymmetric separation over a spinning baseball in a wind tunnel [29]. The seams enhance the thickness of the boundary layer,

which weakens it, causing it to separate sooner than if there were no seams.

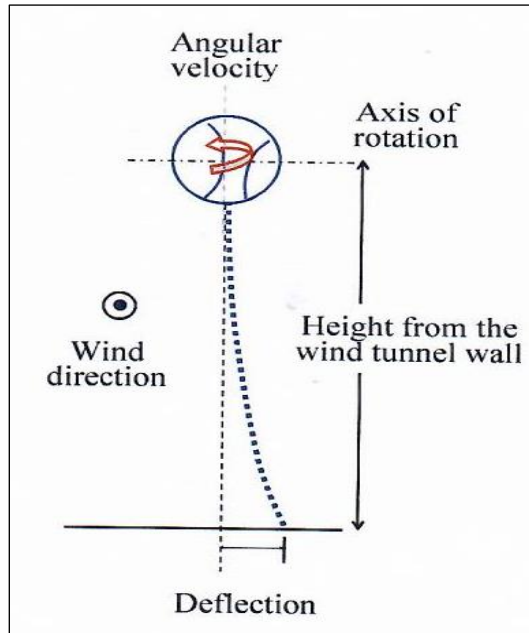


Fig 3: Diagram of Briggs' [29] experimental setup for tests of lateral deflection of baseball in a wind tunnel

**Aerodynamic of forces and moment**

The aerodynamic coefficients and moment are required to simulate trajectory of the soccer ball,

badminton shuttlecock and javelin. Figure 4 shows aerodynamic forces acting on a soccer ball, badminton shuttlecock and javelin.

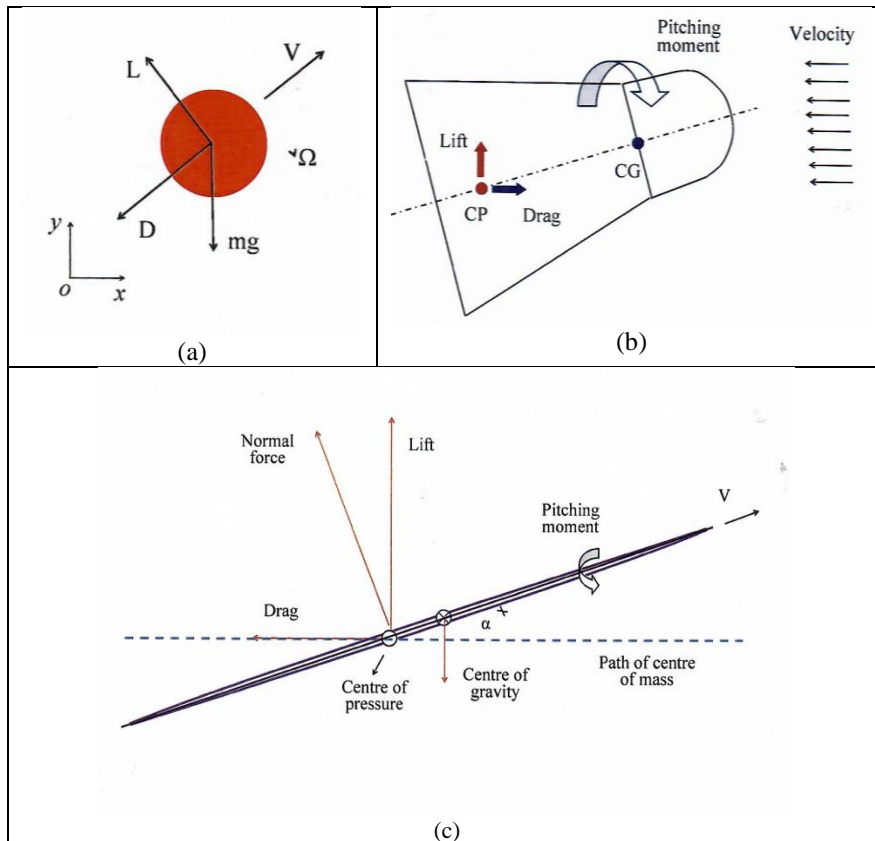


Fig 4: Systematic sketch of aerodynamic forces acting on (a) ball (b) badminton shuttlecock (c) javelin

The aerodynamic forces and moment [15] can be written as:

$$L = N \cos \alpha - A \sin \alpha \dots\dots\dots (1)$$

$$D = N \sin \alpha - A \cos \alpha \dots\dots\dots (2)$$

$$M = T o - N x_0 \dots\dots\dots (3)$$

Where  $L, D, N$  and  $A$  are lift, drag, normal and axial force acting on ball and  $\alpha$  is direction of object direction.  $M$  is the pitching moment. Aerodynamic coefficients of drag and lift coefficient are  $C_D = D / (\frac{1}{2} \rho V^2 S_A)$ ,  $C_L = L / (\frac{1}{2} \rho V^2 S_A)$ , and  $S_A$  is the surface area.  $x_0$  is the distance from position  $o$  on the load cell to the centre of gravity.

We are presenting a dynamic of football, shuttlecock and javelin in flight, highlighting the dominant influence of aerodynamics on their trajectories. The physical parameters of common sports ball is  $r$  and  $m$  correspond to the sport ball's radius and mass respectively,  $V_o$  to its peak speed,  $\Omega$  its spin angular velocity, and  $\mu$  to the molecular viscosity of air. The corresponding dimensionless groups: the range parameter  $A = V_o^2 / (gr)$ , the coefficient of ballistic coefficient, and  $\beta = mg / (\pi a^2 \rho V_o^2)$ . The lower value of ballistic coefficient  $\beta$ , the greater influence of aerodynamic drag effects on the flight of the ball, badminton shuttlecock and javelin. The small value of ballistic coefficient  $\beta$  for most sports indicate that the

aerodynamic drag exerted at peak speed  $V_o$  is typically comparable to or greater than the weight of the ball. Aerodynamic drag coefficient  $C_D$  may depend on the projectile's speed, spin rate, and surface characteristics. Equations of trajectory simulation [40, 41] can be written as:

$$m \frac{d^2x}{dt^2} + D \cos \theta + L \sin \theta = 0 \dots\dots\dots (4)$$

$$m \frac{d^2y}{dt^2} - L \cos \theta + D \sin \theta + mg = 0 \dots\dots\dots (5)$$

The air flowing around the ball is deflected sideways, resulting in an asymmetrical wake behind the ball as shown in Fig 2. The air in the wake has downward or negative momentum. Ballistic coefficient is the ratio of weight to air drag. The ballistic performance indicates how important aerodynamic forces are on the trajectory of a ball in flight. The magnitude and direction of the momentum vector and its corresponding Magnus force [30]. For  $Re < 10^5$ , the Magnus force is conventionally defined positive ( $C_L > 0$ ) for a Reynolds number greater than  $1.28 \times 10^5$ , the sign of the Magnus force negative ( $C_L < 0$ ) for a finite range of spinning velocities. This reversal of the direction of the rotation is known as the reverse Magnus effect [30], and is most likely observed at a very large Reynolds number.

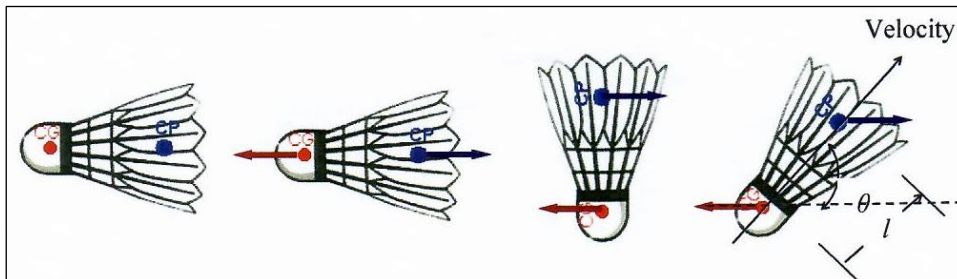


**Fig 5: Representation of aerodynamic forces on shuttlecock**

According to Newton's 3rd law of motion, there is an upward force component called the Magnus force or lift force as shown in Fig. 2. Dimensionless lift coefficient as  $C'_L = C_L / SP$  here the dimensionless parameter is derived by  $SP = r\Omega/V$  which is the ratio of the ball's tangential equatorial speed to its centre-of-mass speed. Here,  $r$  is the ball radius. The lift coefficient is then defined in terms of the ball's spin rate. The aerodynamic coefficients  $C_D$  and  $C_L$  are, in general, complicated functions of ball translation speed, spin rate and properties of the ball's surface.

The shuttlecock is a bluff body and, as such, the predominant drag regime is base drag. The span wise (y-direction) vorticity is given by

$$\omega = \frac{\partial u}{\partial y} - \frac{\partial v}{\partial x} \dots\dots\dots (6)$$

Where  $V$  and  $U$  indicate the velocity in the  $x$  and  $y$  directions, respectively. Figure 5 shows vorticity acting on a badminton shuttlecock. The centre of pressure  $CP$  and centre of gravity  $CG$  are shown with aerodynamic forces. The pitching moment requires length  $l$  and angle of attack of badminton  $\theta$ .

### 3. AERODYNAMIC OF FOOTBALL

The later deflection is caused by spinning ball (soccer, volleyball, baseball, cricket, tennis ball) about an axis perpendicular to the line of flight is customary known as swing, swerve or curve motion. In the next section, we are developing lift over a spinning sphere in an inviscid and incompressible flow.

#### Inviscid and incompressible flow over spinning sphere

Newton [44] described in the year 1671 that a spinning ball deviates in from its flight path and

attributed to the surrounding air caused the deviation of the flight trajectory. Robins [45] has shown the deflection of a musket ball in terms of their spin rate. Magnus [30] demonstrated experimentally that a rotating cylinder experienced a sideways force when mounted perpendicular to direction of flow of air. The observation of the Magnus effect has been credited from Lord Rayleigh [46]. Earlier explanation for the Magnus effect was founded on Bernoulli's theorem [15] based on inviscid and incompressible flow. The normal force acting is caused by a pressure differential between two sides of the sphere, generating the velocity difference due to the rotation. Later on the invention of boundary layer due to viscous flow by Prandtl provides another explanation of the Magnus effect attributed asymmetric and flow separation [17, 18].

Bearman and Harvey [47] have demonstrated that the normal force on a spinning sphere is directly proportional to  $\omega V_\infty$ . Watts and Ferrer [48] have found in the analysis of the aerodynamics of curveball that the normal force over the spinning sphere is consistent with the Kutta-Joukowski theorem [15, 49] that can be related a net circulation of an ideal flow over a two-dimensional object result in a lift force proportional to the product of the freestream velocity and circulation.

Poon *et al.*, [50] have carried out numerical simulation of viscous flow over a stationary and rotating sphere using Fourier-Chebyshev spectral collocation. Numerical simulations used to solve spinning spheres but do not exhibit generalized relation between lift to spinning rate.

The inviscid and incompressible flow past a spinning sphere is derived by superposition of elementary uniform flow and doublet to obtain an

analytical expression as a function of translation speed and rotation velocity. Pressure distribution and lift force over a spinning sphere are obtained applying Kutta-Joukowski theorem [15] with the assumption that the flow field around the spinning sphere may not affect the synthesized flow. The analytical aerodynamic analysis represents that the normal force over the spinning sphere is directly proportional to spinning speed. It also agrees with the experimental data of Bearman and Harvey [42]. The lift force perpendicular to the spinning ball plays significant interest in many sports activities [43] such as baseball, basketball, cricket ball, golf ball, ping pong ball, tennis, football, and volleyball etc, because the balls are having transverse and rotate motion simultaneously and also generates drift from its trajectory.

The focus of this section is to derive an analytical expression for steady, inviscid, incompressible and axisymmetric flow past a spinning sphere. The analysis includes a superimpose of uniform flow with doublet that synthesis of lifting flow over a spinning sphere. It is important to mention here that source, sink and doublet represent three dimensional in nature of fluid mechanics.

A rotating sphere moving through a stream of fluid also experiences a force perpendicular to both the axis of rotation and the motion. It is important to mention here that source, sink and doublet represent three dimensional in nature of fluid mechanics. Figure 6 shows  $r, \varphi, \theta$  are the spherical coordinates. The freestream flow is along the  $z$ -axis and the sphere is constrained to rotate in between the  $y$ -axis and  $z$ -axis. The sphere is constrained to rotate at an angular velocity.

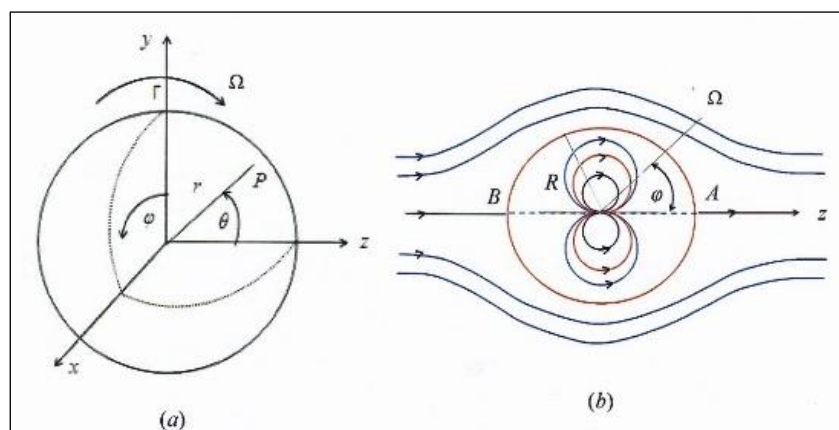


**Fig 6: (a) Spherical polar coordinate system (b) Superposition of a uniform flow and a doublet [49]**

Figure 6 shows a symmetric diagram representing the superposition of uniform flow in the positive  $z$ -direction and with doublet [49]. The doublet is so ordered that the source is placed upstream.

It is important to mention here that the source, sink and doublet represent 3-Dimensional in nature of fluid mechanics, let us consider for a uniform flow and a doublet combination the constant streamline yields the following equation [49] as:

$$\left(r^3 - \frac{\mu}{2\pi V_\infty}\right) \sin^2\theta = 0 \dots\dots\dots (7)$$

$$\phi = V_\infty r \left[ \frac{1}{2} \left(\frac{R}{r}\right)^2 + 1 \right] \cos\theta \dots\dots\dots (11)$$

Where  $\mu$  is the doublet strength with source placed upstream. Equation (7) can be satisfied if either  $\sin\theta = 0$  or  $\theta = 0$  or  $\pi$  and

$$r = \left(\frac{\mu}{2\pi V_\infty}\right)^{\frac{1}{3}} \dots\dots\dots (8)$$

of  $r$  at a point  $A$  and  $B$  as shown in Fig. 6 (b) on the  $z$ -axis the radius of the sphere  $R$  as following

$$R = \left(\frac{\mu}{2\pi V_\infty}\right)^{\frac{1}{3}} \dots\dots\dots (9)$$

Thus,  $\psi_o$  represents the streamline for a sphere of radius  $R$  and the  $z$ -axis. The sphere may be considered as a solid wall as there is no flow across a streamline. Figure 6 (b) shows two stagnation points on the spinning sphere on the  $z$ -axis. They are

$$\left[\left(\frac{\mu}{2\pi V_\infty}\right)^{\frac{1}{3}}, 0\right] \text{ and } \left[\left(\frac{\mu}{2\pi V_\infty}\right)^{\frac{1}{3}}, \pi\right]$$

For  $r > R$ , equations for stream function and velocity potential can be written as

$$\psi = \frac{V_\infty}{2} \left(r^2 - \frac{R^2}{r}\right) \sin^2\theta \dots\dots\dots (10)$$

The velocity components in the radial and tangential directions are

$$V_r = V_\infty \left(1 - \frac{R^3}{r^3}\right) \cos\theta \dots\dots\dots (12)$$

$$V_\theta = -V_\infty \left(1 + \frac{R^3}{2r^3}\right) \sin\theta \dots\dots\dots (13)$$

The velocity components  $v_r$  and  $v_\theta$  are  $0$  and  $-(3/2)V_\infty \sin\theta$ , respectively, at  $r = R$ . The stagnation points occur at  $\theta = 0$  and  $\pi$  and the maximum velocity occurred at  $\theta = \pi/2$  and  $\theta = (3/2)\pi$  with a value of  $|v_\theta|_{\max} = -(3/2)V_\infty$ . The pressure on the sphere can be obtained by employing Bernoulli's equation. The pressure coefficient on the non-spinning sphere is:

$$C_p = 1 - \frac{9}{4} \sin^2\theta \dots\dots\dots (14)$$

The sphere is considered smooth. We have focused here with steady, inviscid and incompressible axisymmetric flow past a sphere, the flow uniform. The lift force exists perpendicular to the flow direction of rotation which depends on the angular velocity of the sphere as well as the direction of the movement.

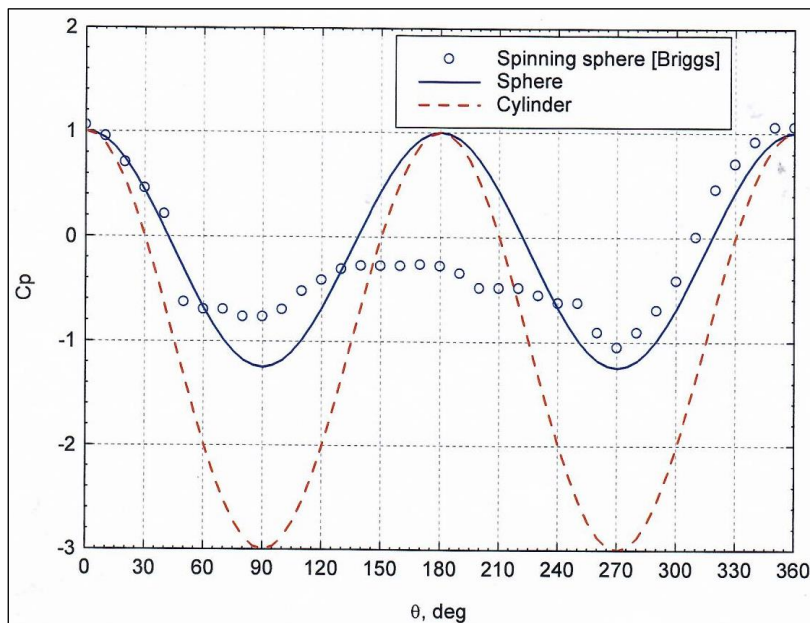


**Fig 7: Pressure variation on non-spinning cylinder, sphere and over spinning sphere [29]**

The pressure distributions over non-spinning cylinder and sphere and experimental data over spinning sphere of Briggs [29] are shown in Figure 7. Briggs measured pressure over a spinning sphere of radius 7.62 cm (3") with a freestream velocity of 38 m/s (125 ft/s) in a wind tunnel. The experimental pressure distribution is of the same quality identical trend as non-spinning sphere but differ attributed viscous effect and spinning of the sphere. The absolute magnitude of the pressure coefficient on a sphere is less than that for

a circular cylinder [15] which is due three-dimensional relieving effect.

We have superimposed the doublet with uniform velocity. The lift over the spinning sphere is obtained integrating pressure on the equatorial plane be written as:

$$L = - \int_0^{2\pi} \left[ \frac{\rho}{2} V_\infty^2 - \frac{\rho}{2} \left( \frac{3}{2} V_\infty \sin\phi + \frac{\Gamma}{2\pi R} \right)^2 \right] R \sin\theta d\theta \dots\dots\dots (15)$$

The integration yields the lift on a spinning sphere in an inviscid flow

$$L = \frac{3}{4} \rho_{\infty} V_{\infty} \Gamma \dots\dots\dots (16)$$

The normal force over spinning cylinder per unit length [15] is  $\rho_{\infty} V_{\infty} \Gamma$ . It reveals that the normal force over the spinning sphere is less than the spinning circular cylinder.

$$V_{\infty} \left( 1 + \frac{R^3}{2r^3} \sin\phi \right) + \frac{\Gamma}{2\pi r} = 0 \dots\dots\dots (17)$$

$$2r^3 - \frac{r^2 \Gamma}{\pi V_{\infty}} + R^3 = 0 \dots\dots\dots (18)$$

The above cubic equation can be written as

$$\alpha^3 + v\alpha + w = 0 \dots\dots\dots (19)$$

Where

$$v = \frac{1}{3} \left( \frac{\Gamma}{2\pi V_{\infty}} \right)^2$$

and

$$w = \frac{2}{27} \left( \frac{\Gamma}{2\pi V_{\infty}} \right)^2 + \frac{1}{2}$$

Three roots [50] of Equation (18) are  $x_1, x_2,$  and  $x_3$  and written as

$$\alpha_1 = A_1 + B_1, \alpha_2, \alpha_3 = -\frac{1}{2}(A_1 + B_1) \pm \frac{\sqrt{3}}{2}(A_1 + B_1)i$$

Where

$$A_1 = \left[ -\frac{w}{2} + \sqrt{\left(\frac{w^2}{4} + \frac{v^3}{27}\right)} \right]^{\frac{1}{3}}$$

$$B_1 = \left[ -\frac{w}{2} - \sqrt{\left(\frac{w^2}{4} + \frac{v^3}{27}\right)} \right]^{\frac{1}{3}}$$

There is one real root and two conjugate complex roots, when

$$\Gamma > 6\pi V_{\infty} \left( \frac{R^3}{2} \right)^{\frac{2}{3}} \dots\dots\dots (20)$$

The tangential velocity component on the surface of the spinning sphere yields a cubic equation which is having one real and two conjugate imaginary roots.

**Viscous flow over spinning sphere**

The viscous flow over sport balls needs detailed studies to account boundary layer effects on fluid mechanics and flight dynamics. A spinning sphere moving through a stream of fluid also experiences a force perpendicular to both the axis of rotation and the motion. The flow structure is considerably more complex as described above.

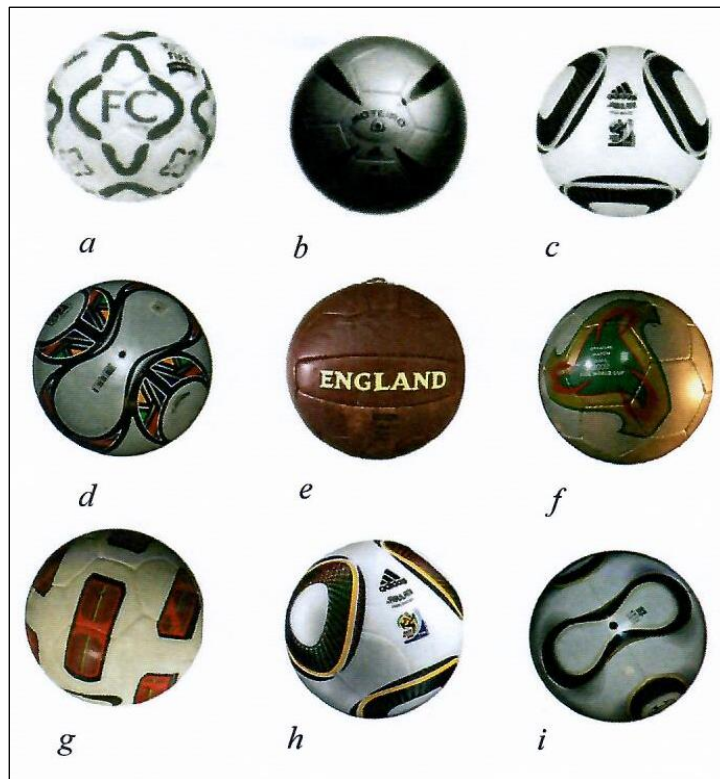


**Fig 8: The evolution of the football (a) 1900, (b) 2001, (c) 2010 WC, (d) 2009, (e) 1966 WP, (f) 2002, (g) 2010 (Nike), (h) 2010 (Nike) and (i) 2006 (WP)**

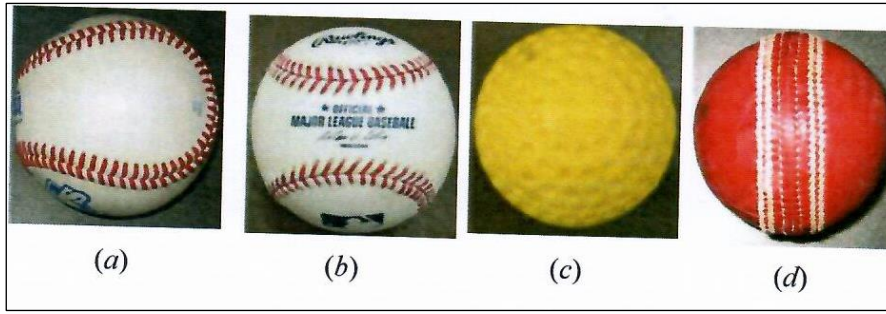


**Fig 9: Sport ball (a) NCAA baseball, (b) MLB baseball, (c) Dimpled golf ball, and (d) cricket ball**

The aerodynamic performance of various sports balls as shown in Figs 8 and 9 was studied by Passmore *et al.*, [51]. Effect of surface geometry and surface structure on soccer balls aerodynamics and trajectories are studied by Barber *et al.*, [37] and Alam

*et al.*, [38], respectively. Table 1 gives weight, radius, peak velocity, Reynolds number, range parameter, ballistic coefficient and spin parameters of various sport balls. The influence of ballistic coefficient on sport balls are discussed in the above section.

**Table 1: Aerodynamic parameters of various sports ball**

| Sport       | $m$ (gm) | $r$ , cm | $V_0$ , (m/s) | Re      | $A$    | $\beta$ | $S$  |
|-------------|----------|----------|---------------|---------|--------|---------|------|
| Basket ball | 630      | 11.9     | 15            | 120,000 | 190    | 0.5     | 0.07 |
| Soccer ball | 430      | 11.3     | 32            | 240,000 | 910    | 0.1     | 0.21 |
| Volley ball | 270      | 10.5     | 30            | 210,000 | 860    | 0.08    | 0.21 |
| Shot put    | 7260     | 6.0      | 10            | 40,000  | 170    | 54      | 0.05 |
| Tennis      | 58       | 3.8      | 70            | 180,000 | 12,000 | 0.22    | 0.19 |
| Base ball   | 150      | 3.66     | 40            | 100,000 | 4,200  | 0.2     | 0.18 |
| Cricket     | 160      | 3.6      | 40            | 100,000 | 4,400  | 0.2     | 0.18 |
| Golf        | 45       | 2.1      | 80            | 110,000 | 30,500 | 0.05    | 0.09 |
| Squash      | 24       | 2.0      | 70            | 100,000 | 24,500 | 0.03    | 0.1  |
| Ping-pong   | 2.5      | 2.0      | 45            | 60,000  | 10,125 | 0.008   | 0.36 |

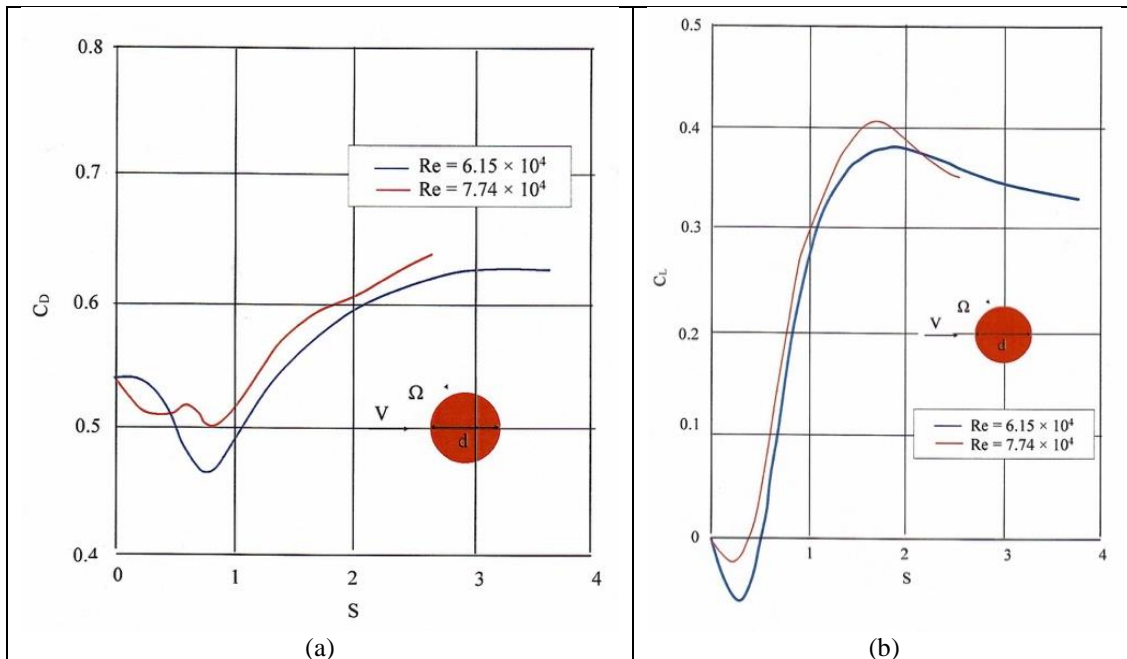


**Fig 10: Variation of lift and drag coefficients on a spinning sphere with the spin parameter**

Kim *et al.*, [52] and Kharlamov *et al.*, [53] have carried out wind tunnel testing to determine if the inverse Magnus effect on a spinning sphere is a function of spin parameters. Figure 10 exhibits

aerodynamic coefficients of  $C_L$  and  $C_D$  for  $Re = 6.15 \times 10^4$  and  $7.74 \times 10^4$ .

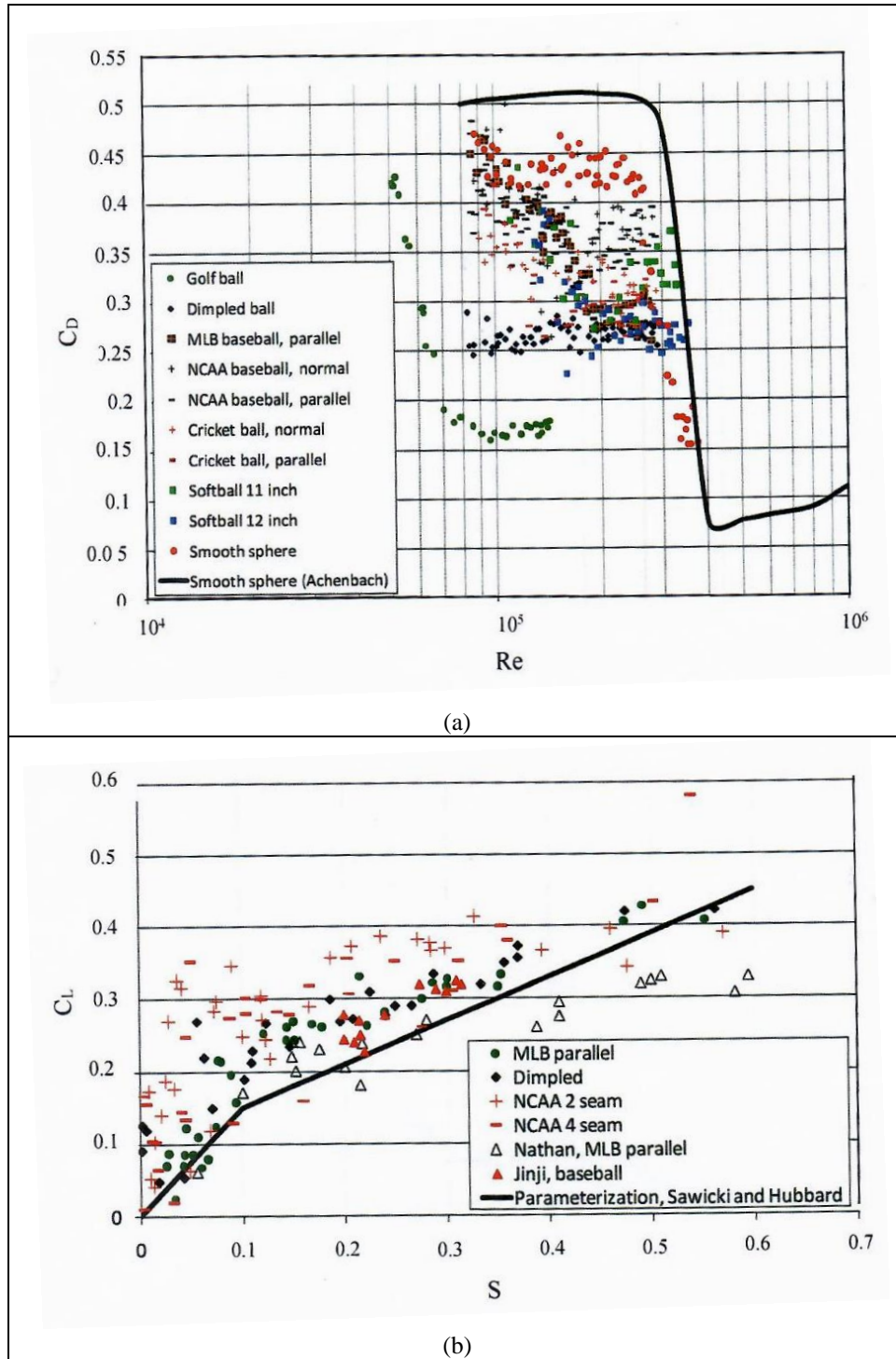


Fig 11: Variation of (a) drag and (b) lift coefficients on a spinning sphere with the spin

Drag coefficients of several spinning sports balls are shown in Fig 11(a) as a function of Reynolds number based on numerical analysis [54] as well as experimental data [55]. Figure 11(b) shows lift coefficient as a function of the spin ratio. The phenomenon of variable lift and drag with spin rate is familiar in golf, baseball, soccer, tennis and ping-pong, the spin rate is used to control the trajectory and bounce of a shot. The spin results in an increase in the lift coefficient.

### Aerodynamics of shuttlecock

A shuttlecock skirt is composed of an array of diverging stems, the ends of which are at the convergent end of the skirt, joined together in an end ring. Figure 12 shows nomenclature and dimension of feather and synthetic badminton shuttlecock. Aerodynamic forces on the badminton shuttlecock are shown in Fig 1(b). Table 2 shows various geometrical parameters of synthetic and feather shuttlecock.

A badminton shuttlecock flies in a high-drag, and thus, the sport has been a subject of research from the point of view of aerodynamics. The small value of ballistic coefficient  $\beta$  indicates the largest in-flight deceleration of spinning sport ball. The ballistic coefficient represents its ability to overcome air resistance in flight and is inversely proportional to deceleration.

The badminton shuttlecock may be considered as a bluff body and the predominant drag mechanism is base drag. Increased porosity does not necessarily

reduce the drag coefficient. The drag coefficients of the feather and synthetic shuttlecock were approximately about 0.48. About 95% of the mass of it is located in the dome-like cork tip. So obviously the centre of gravity  $CG$  will be located near the tip. The centre of pressure  $CP$  is somewhere near the feathers, relatively far back. Figure 5 shows two equal but opposite forces that do not act on one line are equivalent to a torque. the bigger the distance between the  $CP$  and the  $CG$ , the bigger the torque. We have studied experimentally badminton shuttlecocks trajectories with a high-speed camera.

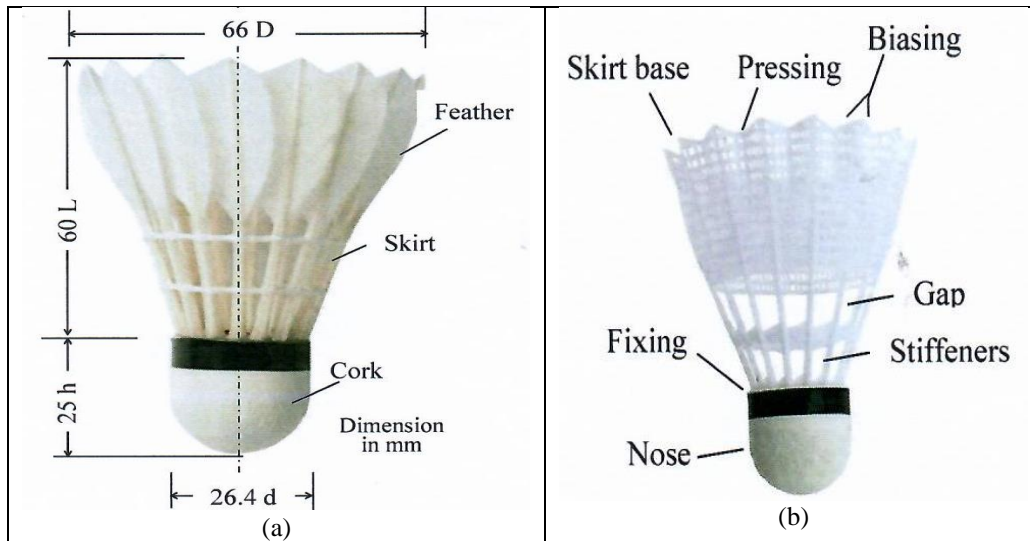


Fig 12: Badminton shuttlecock (a) feather (b) synthetic

Table 2: Aerodynamic parameters of various sports ball

| ID  | Type      | Length of shuttle (mm) | Length of cock (mm) | Width at end Of skirt (mm) | Mass (gm) |
|-----|-----------|------------------------|---------------------|----------------------------|-----------|
| S-1 | Synthetic | 84                     | 25                  | 65                         | 5.2       |
| S-2 | Synthetic | 82                     | 25                  | 63                         | 4.9       |
| S-3 | Synthetic | 83                     | 25                  | 66                         | 6.2       |
| S-4 | Synthetic | 78                     | 25                  | 68                         | 5.3       |
| S-5 | Synthetic | 80                     | 25                  | 65                         | 5.2       |
| F-1 | Feather   | 85                     | 25                  | 66                         | 5.0       |
| F-2 | Feather   | 86                     | 25                  | 65                         | 4.9       |
| F-3 | Feather   | 85                     | 25                  | 66                         | 5.1       |
| F-4 | Feather   | 85                     | 25                  | 65                         | 5.2       |
| F-5 | Feather   | 85                     | 25                  | 65                         | 4.9       |

Computer simulation of shuttlecock trajectories has been carried out by Cooke [41]. Experiments showing the aerodynamic characteristics of Shuttlecock are analysed wind tunnel measurements by Alam *et al.*, [56] and Nakagawa *et al.*, [57]. A multicomponent strain gauge or load cell is used to measure aerodynamic forces for a wide range of parameters.

## 5. AERODYNAMIC ANALYSIS OF JAVELIN

Based on the application of Newtonian mechanics to the javelin flight process, a computerized tool makes it feasible to determine the influence on javelin flight trajectory and distance of the characteristic parameters of the throwing release phase. Figure 4(c) shows the aerodynamic forces acting on a javelin. Equations (3) and (4) can be used to determine trajectory of a javelin in conjunction with aerodynamic forces as in equations. (1) and (2). These differential equations of the javelin flight dynamics are based on

the application of Newton's 2nd law of motion. It is observed that during the flight of the javelin the centre of pressure does not coincide with the centre of gravity, causing a pitching moment as depicted in Fig 4(c). The pitching moment is a variable in numerical simulations. Hubbard *et al.*, [58] have carried out numerical simulation of javelin flight employing experimental aerodynamic data. Maheras [59] considered aerodynamic and flight dynamics to determine the javelin performance. The effect of this rotation and vibration [60] on javelin trajectory and flight distance needs numerical simulations. The effect of the elastic vibrations of the javelin on its trajectory and flight distance may not have a significant influence.

Maryniak *et al.*, [61] and Chiu *et al.*, [62] have developed mathematical models to estimate flight

trajectory and distance that will inline the process of improving the javelin throw. Best *et al.*, [63] and Best *et al.*, [64] developed the initial parameters of the throw, which influence the javelin flight trajectory and range. Jiang and Zhou (65) propose a mathematical model that describes the flight of the javelin, obtaining the data referring to the drag forces, lift and the pitching moment from tests in a wind tunnel.

Numerical simulations can also include ambient conditions, gravitational forces and initial throwing parameters. The mean prediction error obtained during the comparison of the javelin flight distance calculated with the model, with the actual throwing results, ranged from 0.65% to 1.58%.

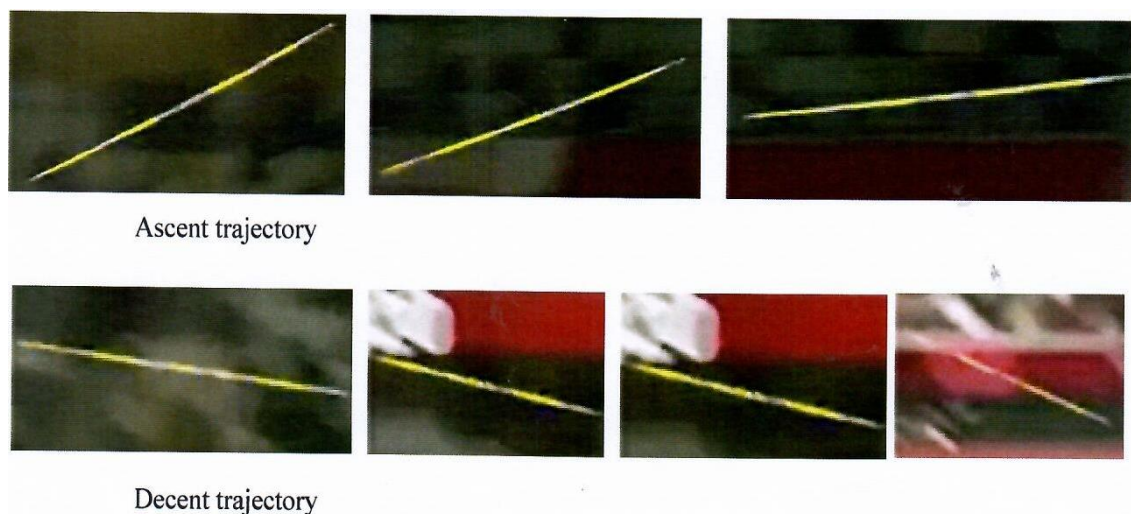


**Fig 13: Trajectory of javelin in ascent and descent phase**

White [6] has studied the optimal coupling between the pitching angle and the projectile velocity to achieve the longest flight trajectory, which may be particularly different for each athlete and that the determination of this indicator is not possible without considering mathematical modelling in conjunction with experimentation.

The length of the javelin varies from 2.5 m (8' 2") – 2.7 m (8' 10"), weight about 800 g (0.363 lb), range about 98.48 m (321' 1") - 90.57 m (297' 1½"), CG about 1.5 m and peak speed about 113 km/h (70 m/h). The CP is located behind the CG. The videos have been calibrated and digitised to study javelin motion taking video camera data [66]. Still images have been captured from video and shown in Fig 13. The above mentioned is used to study the aerodynamic and flight dynamics of javelin.

## CONCLUSION

Analytical aerodynamic analysis is presented by superimposing a uniform flow and doublet to compute the lift over a spinning sphere in an inviscid

flow and incompressible flow. Solution of the ideal flow equation is based on Kutta-Joukowski theorem with the assumption that the flow field around the spinning sphere will not influence the synthesized flow. The tangential velocity component on the surface of the spinning sphere yields a cubic equation which has one real and two conjugate imaginary roots. The lift force over the spinning sphere is directly proportional to circulation velocity which coincide with experimental results of Bearman and Harvey, however, is less than spinning circular cylinder. Mathematical model is described to analysis performance of badminton shuttlecock. Aerodynamic and flight dynamic models are employed in conjunction with still pictures of videos.

## REFERENCES

1. Adair, R. K. (2002). *The Physics of Baseball*. 3<sup>rd</sup> Ed. Perennial Harper Collins, New York.
2. Daish, C. B. (1972). *The Physics of Ball Games*. The English Universities Press Ltd, London.
3. Gay, T. (2005). *The Physics of Football*. HarperCollins, New York.

4. Wesson, J. (2002). *The Science of Soccer*. Institute of Physics Publishing, London.
5. de Mestre, N. (1990). *The Mathematics of Projectiles in Sport*. Cambridge University Press, Cambridge.
6. White, C. (2013). *Projectile Dynamics in Sport. Principles and applications*. Routledge Chapman & Hall Publisher. ISBN 9780415833141
7. Kreighbaum, E., & Barthels, M. (1996). *Biomechanics: A Qualitative Approach for Studying Human Movement*. 4th ed. Allyn and Bacon.
8. Motulsky, H., & Christopoulos, A. (2004). *Fitting Models to Biological Data Using Linear and Nonlinear Regression*, Oxford University Press.
9. Groff, J. E. (2013). A review of recent research into aerodynamics of sport projectiles, *Sports Eng*, 16, 137–154. DOI 10.1007/s12283-013-0117-z
10. Mehta, R. D., & Pallis, J. M. (2001). Sports ball aerodynamics: Effects of velocity, spin and surface Roughness. *Materials and Science Sports*, ed. Froes EH, S. J., Haake, S. J. TIMIS 184 Thorn Hill Road Warrendale, PA, USA. 185-197.
11. Mehta, R. D. (1985). The aerodynamics of sports balls. *Annual Review of Fluid Mechanics*, 17, 151–189.
12. Mehta, R. D., Alam, F., & Subic, A. (2008). Aerodynamics of tennis balls- a review. *Sports Technology*, 1(1), 1-10.
13. Maszczyk, A., Zaja, C. A., & Ryguła, I. (2011). A neural network model approach to athlete selection. *Sports Eng*, 13, 83–93.
14. Johnson, N., & Chae, E. J. (2020). 2D aerodynamic analysis of a badminton shuttle for re-entry vehicle applications. Proc. SPIE 11376, Active and Passive Smart Structures and Integrated Systems XIV, 1137615. <https://doi.org/10.1117/12.2558935>
15. Anderson, J. D. (1985). *Fundamentals of Aerodynamics*, International Student Edition, McGraw-Hill Book Company Singapore.
16. Anderson, J. D. (2005). *Introduction to Flight*. 5<sup>th</sup> Ed. McGraw – Hill International Edition Singapore.
17. Prandtl, L. (1952). *Essentials of Fluid Dynamics*, Hafner Publishing Company, New York.
18. Schlichting, H. (1960). *Boundary Layer Theory*. 4<sup>th</sup> Ed. McGraw – Hill Book Co.
19. Hoerner, S. F., & Borst, H. V. (1985). Fluid-Dynamic Lift. Information on Lift and its Derivatives, in *Air and in Water*. Hoerner Fluid Dynamics.
20. Hoerner, S. F. (1951). *Aerodynamic Drag*, Otterbein Press, Dayton, Ohio.
21. Achenbach, E. (1974). The effects of surface roughness and tunnel blockage on the flow past spheres. *J Fluid Mech*, 65, 113-125.
22. Achenbach, E. (1972). Experiments on the flow past spheres at very high Reynolds numbers. *Journal of Fluid Mechanics*, 54, 565–575.
23. Fuss, F. K., Smith, R. M., & Subic, A. (2012). Determination of spin rate and axes with an instrumented cricket ball. *Proc Eng*, 34, 128–133.
24. Davies, J. M. (1949). The aerodynamics of golf balls. *American Journal of Physics*, 20, 821-828.
25. Ou, K., Castonguay, P., & Jameson, A. (2011). Computational sports aerodynamics of a moving sphere: Simulating a ping pong ball in free flight, AIAA 2011-3668.
26. Alam, F., Chowdhury, H., Theppadungporn, C., & Subic, A. (2010). Measurements of aerodynamic properties of badminton shuttlecocks. *Proc Eng*, 2, 2487–2492.
27. Rae, W. J., & Steit R. J. (2002). Wind-tunnel measurements of the aerodynamic loads on an American football. *Sport Eng*, 5, 165–172.
28. Maccoll, J. W. (1928). Aerodynamics of a spinning sphere. *Journal of the Royal Aeronautical Society*, 32, 777–798.
29. Briggs, L. J. (1959). Effect of Spin and Speed on the Lateral Deflection (Curve) of a baseball; and the Magnus effects for Smooth Spheres. *American Journal of Physics*, 27, 589-596.
30. Magnus, G. (1851). Ueber die abweichung der geschosse, und: Ueber eine auffallende erscheinung bei rotirenden korpern. *Annalen der Physik*, 164, 1-29.
31. Hanna, R. K. (2012). CFD in sport - a retrospective; 1992-2012,” *Procedia Engineering*, 34, 622–627.
32. Barber, S., Chin, S. B., & Carré, M. J. (2009). Sports ball aerodynamics: A numerical study of the erratic motion of soccer balls. *Computers & Fluids*, 38, 1091-1100.
33. Jalilian, P., Kreun, P. K., Makhmalbaf, M. M., & Liou, W. W. (2014). Computational aerodynamics of baseball, soccer ball and volleyball. *American Journal of Sports Science*, 2, 115-121. doi: 10.11648/j.ajss.20140205.12
34. Iftikhar, S., Sherbaz, S. H. A., Sehole, H., Maqsood, A., & Mustansar, Z. (2022). Large Eddy Simulation of the Flow Past a Soccer Ball. *Mathematical Problems in Engineering*, Article ID 3455235, 13. <https://doi.org/10.1155/2022/3455235>
35. Poon, K. W., Ooi, A., Giacobello, M., Peralta, C., & Melatos, A. (2007). Numerical simulation of flow past a stationary and rotating sphere. 16th Australasian Fluid Mechanics Conference. *Australia*, 870-875p.
36. Verma, A., Desai, A., & Mittal, S. (2013). Aerodynamics of badminton shuttlecocks. *J Fluid Struct*, 41, 89-98.
37. Barber, S., & Carre, M. J. (2010). The effect of surface geometry on soccer ball trajectories. *Sports Eng*, 13, 47–55.
38. Alam, F., Chowdhury, H., Stemmer, M., Wang, Z., & Yang, J. (2010). Effects of surface structure on soccer ball aerodynamics, 9th Conference of the International Sports Engineering Association (ISEA).

39. Griffiths, I., Evans, C., & Griffiths, N. (2005). Tracking the flight of a spinning football in three dimensions. *Measurement Science and Technology*, 16, 2056–2065. doi:10.1088/0957-0233/16/10/022
40. Chen, L. M., Pan, Y. H., & Chen, Y. J. (2009). A study of shuttlecock's trajectory in badminton. *J Sports Sci Med*, 8, 657–662.
41. Cooke, A. J. (2002). Computer simulation of shuttlecock trajectories. *Sports Eng*, 5, 93–105.
42. Bearman, P. W., & Harvey, J. K. (1976). Golf ball aerodynamics. *Aeronautical Quarterly*, 21, 112–122.
43. Goff, J. E. (2010). Power and spin in the beautiful game. *Phys Today*, 63, 62–63.
44. Newton, I. (1971). New Theory about Light and Colours, Philosophical Transactions of the Royal society, 6, 3078.
45. Robins, B. (1742). *New Principles of Gunnery*, Hutton, London.
46. Lord, R. (1877). On the irregular flight of a tennis ball. *Messenger of Mathematics*, 7, 14–16.
47. Bearman, P. W., & Harvey, J. K. (1976). Golf ball Aerodynamics, *Aeronautical Quarterly*, 21, 112–122.
48. Watts, R. G., & Ferrer, R. (1987). The lateral force on a spinning sphere. *American Journal of Physics*, 55, 40–45.
49. Yuan, S. W. (1969). *Foundations of Fluid Mechanics*. Prentice-Hall of India Private Limited, New Delhi, India.
50. Grewal, B. S. (2014). *Higher Engineering Mathematics*. 43<sup>rd</sup> ed. Khanna Publishers, Delhi, India, 49-50p.
51. Passmore, M., Rogers, D., Tuplin, S., Harland, A., Lucas, T., & Holmes, C. (2022). The aerodynamic performance of a range of FIFA approved footballs. *Proc Mech Engr Part P*, 226, 134-142. <http://dx.doi.org/10.1177/17543371111415768>
52. Kim, J., Park, H., Choi, H., & Yoo, J. Y. (2013). Inverse Magnus Effect on a Rotating Sphere, *International Symposium on Turbulence and Shear Flow Phenomena*, Poitiers, France.
53. Kharlamov, A., Chára, Z., & Vlasák, P. (2008). Experimental investigation of Magnus Force acting on smooth sphere at high Reynolds numbers, *Colloquium Fluid Dynamics*. Institute of Thermomechanics AS CR. Prague.
54. Alaways, L. W. (1998). *Aerodynamics of the curve ball: An investigation of the effects of angular velocity on baseball trajectories* [thesis]. University of California, Davis.
55. Kensrud, J. R. (2010). *Determining aerodynamic properties of sports balls in situ* [thesis]. Washington State University.
56. Alam, F., Chowdhury, H., Theppadungporn, C., & Subic, A. (2010). Measurements of aerodynamic properties of badminton shuttlecocks. *Proc Eng*, 2, 2487–2492.
57. Nakagawa, K., Hasegawa, H., Murakami, M., & Obayashi, S. (2012). Aerodynamic properties and flow behavior for a badminton shuttlecock with spin at high Reynolds numbers. *Proc Eng*, 34, 104–109.
58. Hubbard, M., & Rust, H. J. (1984). Simulation of javelin flight using experimental aerodynamic data. *J Biomech*, 17, 769–776.
59. Maheras, A. V. (2013). *Basic javelin aerodynamics and flight characteristics*. *Techniques for Track & Field and Cross Country*, 7, 31-41.
60. Hubbard, M., & Bergman, C. D. (1989). Effect of vibrations on javelin lift and drag. *Int J Sport Biomech*, 5, 40–59.
61. Maryniak, J. E., Ładyżyńska-Kozdraś, E., & Golińska, E. (2009). Mathematical modelling and numerical simulations of javelin throw. *Human Movement*, 10, 16–20. DOI:10.2476/v10036.4009.0003.5
62. Chiu, C. H. (2009). Discovering optimal release conditions for the javelin world record holders by using computer simulation. *International Journal of Sport and Exercise Science*, 1, 41-50.
63. Best, R. J., Bartlett, R. M., & Morriss, C. J. (1993). A three-dimensional analysis of javelin throwing technique. *Journal of Sports Sciences*, 11(4), 315–328.
64. Best, R. J., Bartlett, R. M., & Sawyer, R. A. (1995). Optimal javelin release, *J Appl Biomech*, 11, 371–394. DOI: 10.1123/jab.11.4.371.
65. Jiang, M., & Zhou, J. H. (2014). Optimization calculation of javelin throwing results. *Applied Mechanics and Materials*, 716-717, 764-766.
66. Neeraj, C. (2020). Kalinga Stadium, Bhubaneswar, India. Dec. 5, 2020, [www.odishatv.in](http://www.odishatv.in)